Finite-Difference Time-Domain Analysis of Tapered Photonic Crystal Fiber

M.I. Md Ali[1], S. N.Sanusidin[1] and M. H. M. Yusof[2]

[1]*Faculty of Electrical Engineering*
[2]*Faculty of Applied Science*
University Teknologi MARA
40450 Shah Alam, Selangor

Email: masiz135@salam.uitm.edu.my

Abstract— This paper brief about the simulation of tapered photonic crystal fiber (PCF) LMA-8 single-mode type based on correlation of scattering pattern at wavelength of 1.55 μm, analyzation of transmission spectrum at wavelength over the range of 1.0 until 2.5 μm and correlation of transmission spectrum with the refractive index change in photonic crystal holes with respect to taper size of 0.1 until 1.0 using Optiwave simulation software. The main objective is to simulate using Finite-Difference Time-Domain (FDTD) technique of tapered LMA-8 PCF and for sensing application by improving the capabilities of PCF without collapsing the crystal holes. The types of FDTD techniques used are scattering pattern and transverse transmission and principal component analysis (PCA) used as a mathematical tool to model the data obtained by MathCad software. The simulation results showed that there is no obvious correlation of scattering pattern at a wavelength of 1.55 μm, a correlation obtained between taper sizes with a transverse transmission and there is a parabolic relationship between the refractive index changes inside the crystal structure.

Keywords— tapered, photonic crystal fiber, scattering pattern, transmission spectrum, optiwave

1. Introduction

Photonic crystals (PCs) have attracted much attention in the past two decades [1], [2]. It has become a key issue in material engineering to control the optical properties of materials. PCs are materials which have a periodic dielectric constant in three- orthogonal spatial directions. Based on variation in refractive index, PCs are classified as one-dimensional (1D), two- dimensional (2D) and three-dimensional (3D). Fig. 1(a-c) show the schematic illustrations for PCs where yellow colour indicate permittivity, ε at high region and pink colour indicate ε at low region.

A complete band gap along all dimensions in space can be best realized in a 3D system in principle. However, 3D crystals with band gaps in the optical regime prohibit the progression of many applications which lead to the difficulty in fabricating. On the other hand, 2D PCs have been extensively studied because they provide the possibility to control the propagation of light yet remain comparatively easy to fabricate [3-5].

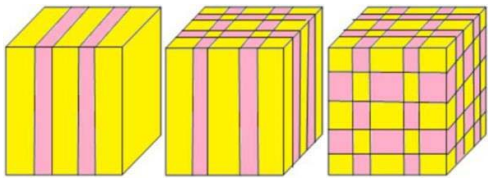

(a) (b) (c)

Figure 1(a-c): From left: 1D-periodic in one direction, 2D-periodic in two directions and 3D-periodic in three directions

FDTD method has been developed and applied to the analysis and investigation of PCs [6-8]. By using an adaptive finite element method in time domain, 2D PC in-plane light propagation is investigated in this work. In the simulation model, both the transverse electric (TE) and transverse magnetic (TM) modes are considered as the polarization characteristics. The PCs' dielectric function profile is discretizing by employed a finite-element method and calculating the in-plane band structures by applying eigenvalue equations with proper periodic boundary conditions following the Bloch theorem [9], [10]. A 2D PC is periodic in two directions (*x,y*) and homogeneous in the third (*z*). For light propagating in the *xy*-plane, we can separate the modes into two independent polarizations, TM and TE modes, and consider the band structure and photon density of states of each. The propagation properties of TM and TE modes can be characterized by the field components parallel to the rods, *Ez*(*x,y*) and *Hz*(*x,y*), respectively as show in Fig. 2.

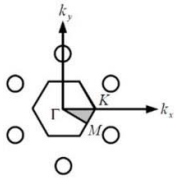

Figure 2: The corresponding reciprocal lattice with irreducible Brillouin zone

PCF is a new dielectric structure with a refractive index that varies periodically in the transverse plane, with a period of the order of an optical wavelength [11]. PCFs or known as microstructured optical fibers (MOFs) are dielectric optical waveguides having a complex air-silica cross-section. Due to the novel optical properties, silica PCFs, also known as holey fibers (HFs) have received considerable attention. By varying the size of air-holes, their number and position, PCF structure can be designed with desirable anomalous group velocity dispersion and modal properties [13][14]. All-silica fiber consist of a solid core with the absence of an air-hole at the lattice site forms a region of raised refractive index, which is surrounded by microstructured cladding, that are typically hexagonally packed, with pitch, Λ (natural length of separation between the two nearest air-holes) and *d*, the air-hole diameter [15], [16] as can be observed in Fig. 4.

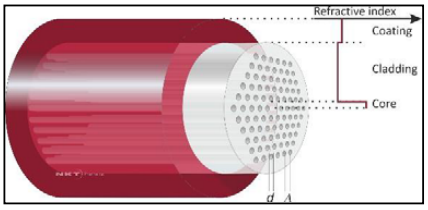

Figure 3: Schematic of an index guided PCF [16]

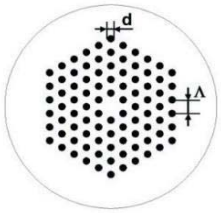

Figure 4: Cross section of triangular cladding PCF [15] [16]

Index guiding (IG) PCFs are made of undoped silica that provides very low losses, sustains high powers and temperature levels, and may withstand nuclear radiation [16]. Fig. 3 shows the IG of a waveguide consists of a solid core and a cladding with an array of air holes. The guided modes may be trapped in a core with a higher refractive index than an averaged index of the cladding. IG is guiding light by total internal reflection between a solid core and a cladding region with multiple air- holes. IG possess the especially attractive property of great controllability in chromatic dispersion by varying the hole diameter and hole-to-hole spacing [17], [18].

In this project, LMA-8 is chosen due to its commercially available. LMA-8-ultraviolet (UV) from NKT Photonics has a hexagonal lattice of air holes surrounding a solid core. LMA-8- UV is a custom fiber made from high-OH fused silica (Heraeus Quarzglas F110), with a core size of 8.6±0.5 *mm* and a cladding diameter of 240±2 *mm*. The cladding diameter of this fiber is larger than that of typical single-mode fibers; this reduces micro-bending, which can increase propagation losses at short wavelengths [19]. An optical micrograph of the fiber cross- section for LMA-8-UV is shown in Fig. 5 [20].

From manufacturer's data, LMA-8 having Λ=5.6 μm and d/Λ=0.49 [21], [22], [23]. The results of LMA-8 PCF tapering are presented in this paper. The focus of the paper is on describing fundamental properties of tapered PCFs, characterization techniques that probe the air-hole collapse looking at the different index.

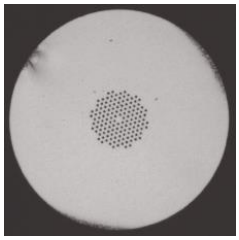

Figure 5: An optical micrograph of the cleaved facet of an uncollapsed LMA-8- UV fiber. The pattern of holes which forms the PC can be seen in the centre. The guided mode propagates through the solid core in the centre of the array of holes [20]

The paper is structured as follows: In Sect. II, the principle of tapering optical fibers are reviewed, and in particular, tapering of PCFs. The air-hole structure of PCF can be well maintained during tapering under certain conditions is demonstrated and a non-destructive method of probing and profiling the PCF microstructure along the taper are described. In Sec. III, the results and discussions of three main objectives are presented and discussed to correlate the scattering pattern of tapered LMA-8 at wavelength of 1.55 μm, to analyse the transmission spectrum of tapered LMA-8 at wavelength over the range of 1.0 until 2.5 μm and to correlate the transmission spectrum with the refractive index change in PC holes with respect to taper size of 0.1 until 1.0. In Sec IV, an overall conclusion of the objectives are concluded and suggested recommendations are listed to achieve the objectives.

2. Methodology

The fiber taper geometry schematic is shown in Fig. 6. A standard flame brushing technique [24], in which the fiber is brushed with a butane flame while simultaneously stretched by motorized stages was applied. In the heated section of the fiber the viscosity decreases and the glass is allowed to flow during this process [25].

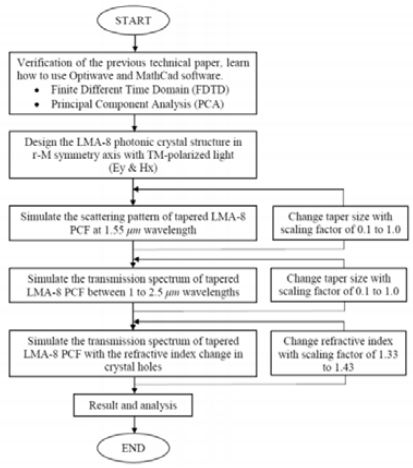

Figure 6: The methodology flow chart

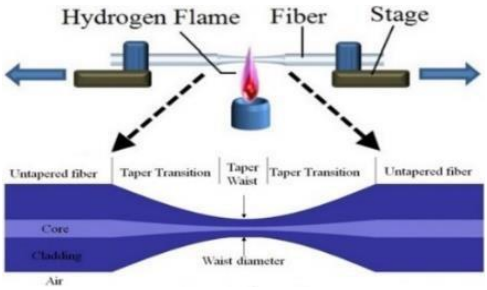

Figure 7: Schematic of a fiber tapering rig

The examination of the PCF microstructure has required the fiber to be cleaved for scanning electron microscope (SEM) analyses in the past. This process is time-consuming, destroys the taper and is most inappropriate for examination of the longitudinal variation in the microstructure although it yields accurate results [21]. Therefore, a novel transverse probing technique is used to analyze the internal structure along the PCF taper, non-destructively [25], [26], [27].

The periodic nature of the PCF microstructure is exploited and the transverse probing technique is illustrated in Fig. 7. The PCF is sandwiched between two butt-coupled SMFs, coupled to a broadband source and an optical spectrum analyzer (OSA), and a transmission spectrum is measured transversely across the PCF. The PCF is sandwiched between two butt-coupled SMFs, coupled to a broadband source and an optical spectrum analyzer (OSA), and a transmission spectrum is measured transversely across the PCF.

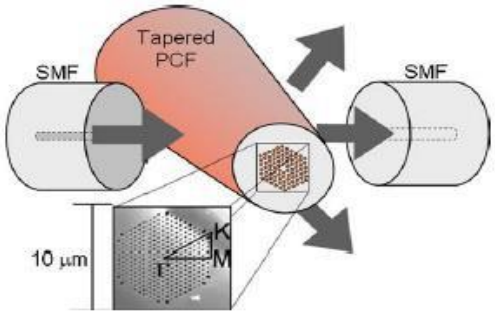

Figure 8: Schematic of the transverse probing technique. The tapered PCF is sandwiched between two SMFs, and the transmission is measured transversely across the taper [25]

Along the taper, the transverse transmission spectra are measured across different positions then in the pitch, the longitudinal variation can be profiled. In the transmission spectrum, the spectral features of PC microstructure are directly linked to the pitch, diameter and regularity of the holes which gives rise to partial photonic bandgaps [28]. By relating the measured bandgap wavelengths to the photonic band structure of the uniform array of holes, the local pitch can be inferred [29] obtained with plane wave expansion (PWE) calculations [25]. By measuring the transverse transmission spectra across different positions along the taper, the longitudinal variation in the pitch can be profiled.

The purpose of simulating and collecting data using Optiwave simulation software over the taper size of 0.1 to 1.0 is to characterize the non-destructive technique. In this case, for an initial experiment, it is crucial to creating a taper size chart to categorize the spectrum pattern but first, we need to cut the PCF as the starting point or reference to correlate between the spectrum and its actual size. The actual size can be determined by using scanning electron microscope (SEM).

This technique is used to ensure the simulation is consistent with the results reported in [25]. The next step is to do PCA and smoothing method using MathCad software. PCA is a technique used to emphasize variation and bring out strong patterns in a dataset and often used to make data easy to explore and visualize [30] meanwhile smoothing method is used to eliminate the noise so that the pattern will not be cluttered

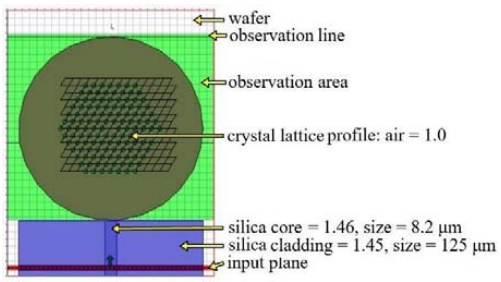

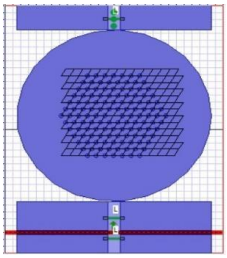

Indices	Material
1.33	Pure Water
1.34	Seawater
1.35	Milk
1.36	Ethyl Alcohol
1.37	Acetic Acid
1.38	Sugar Solution (30%)
1.39	Kerosene
1.40	Octane
1.41	Decane
1.42	Sugar Solution (50%)
1.43	Ethylene Glycol

(a) (b) (c)

Figure 9: (a) The scattering pattern design, (b) the transmission spectrum design of 2D photonic crystal structure measured along the Γ-M direction using Optiwave simulation software, (c) the material of refractive index

As to achieve the second objective on the simulation of transmission spectrum, Bragg's Law equation is used due to constructive interference occurred. The equation is shown in Fig. 9(d) where the calculation is in μm, where λ is wavelength, n is an integer, d is a lattice spacing, and we used maximum sin value of 1 respectively. When x-rays are scattered from a crystal lattice, peaks of scattered intensity are observed which correspond to the following conditions:

- The angle of incidence = angle of scattering.
- The path length difference is equal to an integer number of wavelengths.

The condition for maximum intensity contained in Bragg's law above allow us to calculate details about the crystal structure, or if the crystal structure is known, to determine the wavelength of the x-rays incident upon the crystal.

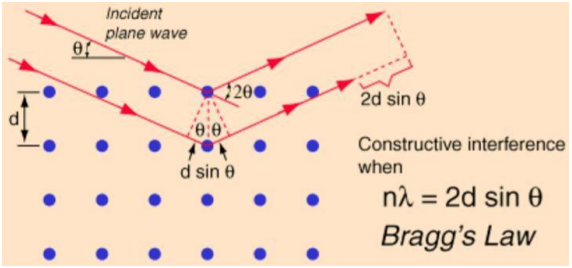

Figure 9: (d) The Bragg's Law illustration and formula

3. Results and Discussions

Scattering is a technique used to observe the quality of the crystal inside LMA-8, meanwhile scattering pattern is pattern observed at a single wavelength. The first objective is to investigate the correlation of scattering pattern of tapered LMA-8 between taper ratios of 0.1 to 1.0 at a wavelength of 1.55 μm. The wavelength of 1.55 μm is chosen due to telecommunication wavelength.

Fig. 10(a-b) shows the scattering pattern measured along r-M symmetry axis (Fig. 8) with TM-polarised light at a wavelength of 1.55 μm where the x-axis is a spatial distance (μm) and the y-axis is the scattering (dB) respectively.

Fig. 10(a-b) shows there is no obvious correlation pattern between the scattering of tapered LMA-8 and taper ratio and Fig. 10(c-d) illustrated the observation area of Ey and Hx scattering pattern respectively from the Optiwave simulation software. PCA used to look at the correlation between the different pattern and Fig. 10(e-f) shows there is no trend and uncluttered PCA of both Ey and Hx respectively. All in all, it can be concluded that when LMA-8 is tapered, there is no relationship in the pattern, no bandgap and uncluttered PCA with respect to taper ratio. Hence, this scattering technique is not suitable to do at the internal structure of LMA-8.

Table 1. Taper ratio indication from 0.1 to 1.0

Taper Ratio	Legend
0.1	
0.2	
0.3	
0.4	
0.5	
0.6	
0.7	
0.8	
0.9	
1.0	

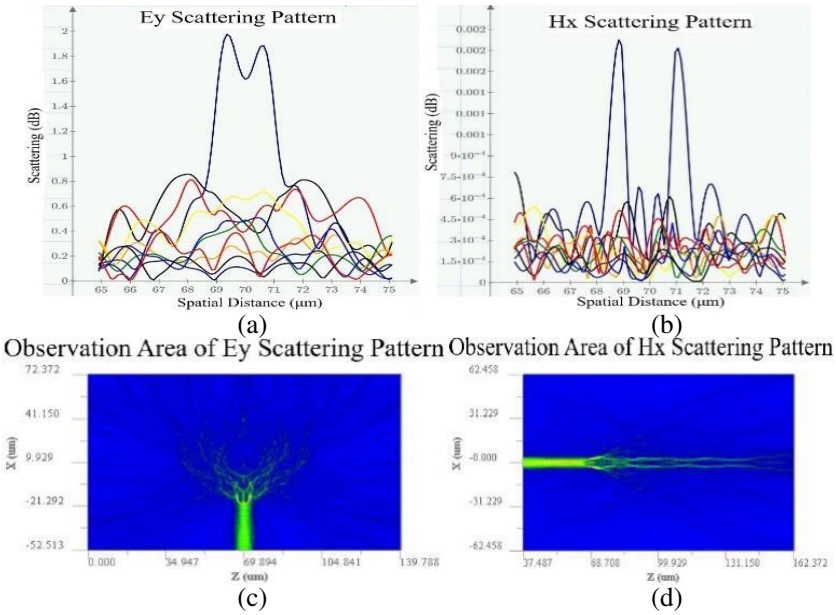

Figure 10 (a) Ey scattering pattern (b) Hx scattering pattern (c) (c) The observation area of Ey scattering pattern, (d) the observation area of Hx scattering pattern from the Optiwave simulation software

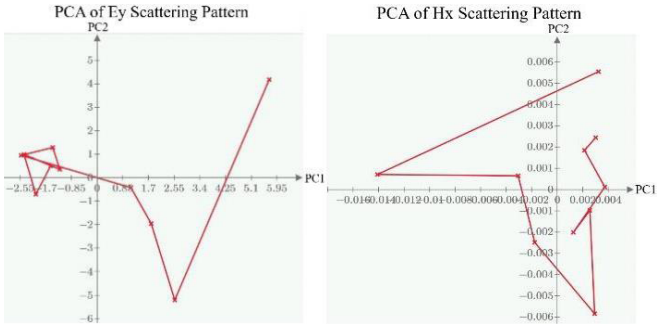

(e) (f)

Figure 10: (e) The PCA of Ey pattern, (f) the PCA of Hx pattern

The second objective is to analyze the transmission spectrum of tapered LMA-8 at a wavelength over the range of 1.0 until 2.5 μm. This can be done by first verification of previous technical paper [25] as shown in Fig. 11(a-b) to ensure the simulation is correct, then we proceed to analyze whether this transmission technique can be applied to LMA-8 or not. Fig. 11(a-b) shows the correct verification of the transverse transmission spectra of the LMA-8 PCF measured along the r- M symmetry axis (as in Fig. 8) with TM-polarised light with taper ratio over the range of 0.40 to 0.75 where x-axis represent the wavelength (μm) and the y-axis represents the transmission (dB).

The PCF has a hole diameter-to-pitch ratio d/Λ of 0.70 and an initial pitch Λ of 1.28 μm. The bandgap shifts to shorter wavelength with decreasing taper size which is similar to the result of previous technical paper [25]. In this case, the bandgap shows that there is no transmission over the wavelength of 1 to 2.5 μm. This is because the holes size, period and pitch are exceptionally small. The purpose of showing the transverse transmission spectra is to prove the fact that we can characterize the taper ratio through transverse transmission using the non- destructive technique without the need to cut the fiber by transversing the light across the LMA-8 PCF, the percentage and position of the point where the light can be transverse can be acquired. Fig 11 (b) illustrates that there is an obvious correlation between the transmission spectrum of previous technical paper with taper size. The similar result was obtained in LMA 8.

Table 2. The indication of taper ratio of 0.4 to 0.75 respectively

Taper Ratio	Legend
0.40	
0.45	
0.50	
0.55	
0.60	
0.65	
0.70	
0.75	

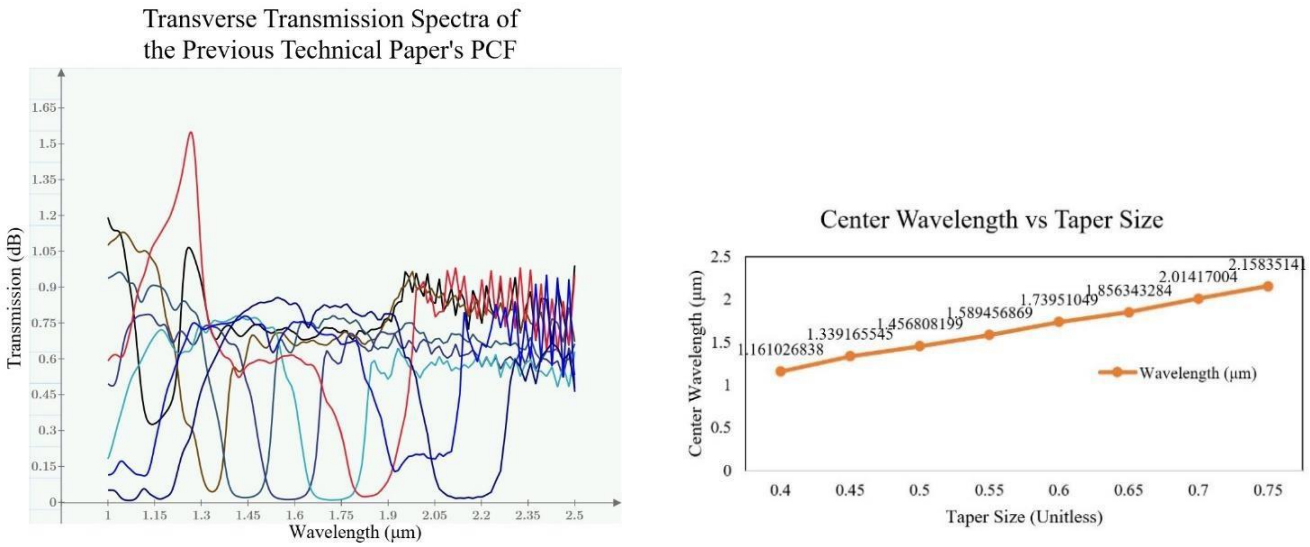

(a) (b)

Figure 11: (a) The transverse transmission spectra of previous technical paper with 0.03 smoothing (b) The graph of center wavelength vs taper size

Fig. 12(a-c) illustrates the transverse transmission spectra of tapered LMA-8 measured along the Γ-M symmetry axis (refer to Fig. 7) with TM-polarised light at wavelength over the range of 1.0 until 2.5 *μm* with respect to taper size of 0.2, 0.3 and 0.5 respectively where the x-axis is the wavelength (*μm*) and y-axis represent the transmission (dB). The selection of wavelength range between 1.0 to 2.5 *μm* is due to the wavelength range of optical spectrum analyzer (OSA) inside the laboratory.

By applying the Bragg's Law, there is a correlation between the transmission spectrum of tapered LMA-8 with taper size. The bandgap wavelength was observed at a longer wavelength. Bandgap transmission occurred when there is no transmission and a reflection at the wavelength. It can be discussed that as the taper ratio increased, the bandgap moves towards a longer wavelength which is known as a red or infrared shift in terms of sensor. But if the bandgap move towards shorter wavelength, it is known as blue shift. This is because the crystal size and pitch of LMA-8 is double than the previous technical paper which is 5.6 *μm* pitch value and 0.49 d/λ value. To be concluded, the transmission spectrum technique is possible to characterize and correlate LMA-8 crystal with taper size.

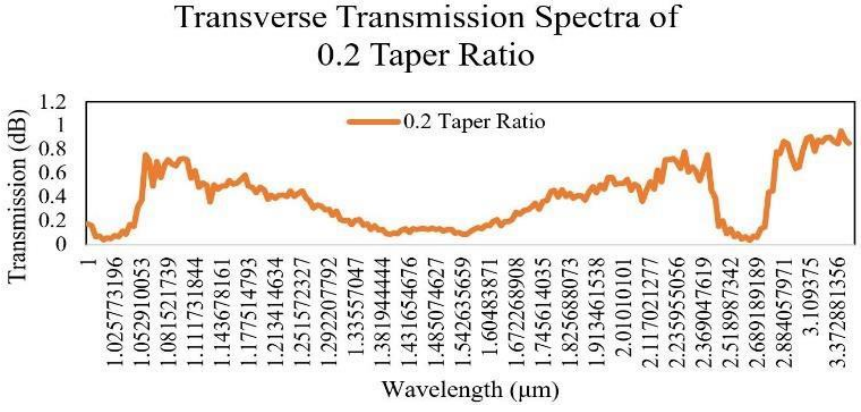

(a)

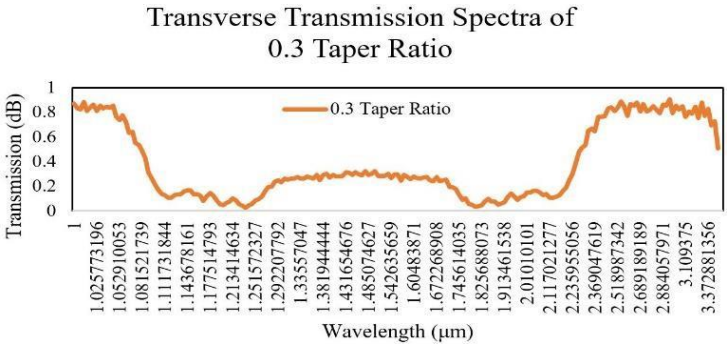

(b)

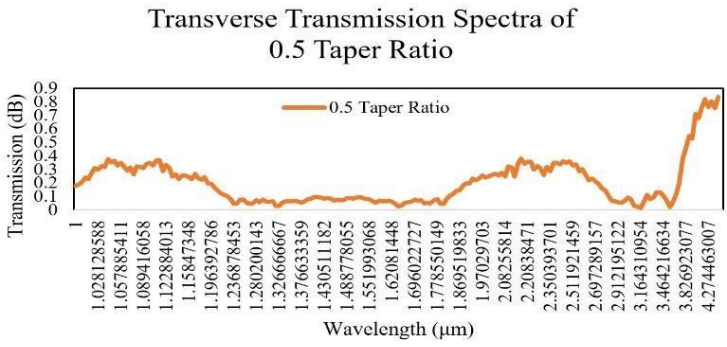

(c)

Figure 12: (a) The transverse transmission spectra of LMA-8 tapered at (a) 0.2 taper ratio observed a total of 3 bandgap(b) 0.3 taper ratio observed a total of 2 bandgap (c) 0.5 taper ratio observed a total of 2 bandgap

The third objective is to correlate the transmission spectrum of tapered LMA-8 with the refractive index change from 1.33 to 1.43 in photonic crystal holes with respect to taper size of 0.1 until 1.0. Fig. 13(a-b) illustrates the correlation of transmission spectra of LMA-8 measured along the Γ-M symmetry axis (as shown in Fig. 2) with TM-polarised light where x-axis represent the wavelength (μm) and the y-axis represents the transmission (dB) tapered at 0.5 and 1.0 respectively. Normally in sensing, the refractive index of distilled water which is 1.33 being used as a standard. We want to investigate on how much power being transferred at different taper size and refractive index from 1.33 to 1.43. The reason on the selection range of refractive index is because we do not want the LMA-8 to be a high-power rod-type PCF and used for correlating material inside the crystal.

To be concluded, there is a relationship between the transmission spectra with respect to taper ratio and there is a pattern on PCA (Fig. 13(c-d)). The two ways to analyze the relationship between the transmission spectrum with refractive index change in LMA-8 PCF holes are multispectral analysis and single spectra at 1.0, 1.5 and 1.9 μm wavelength. The multispectral analysis is analyzing and comparing the whole spectrum by using PCA. We observed that there is a trend between the index of the crystal holes with the value of principal component (Fig. 13(a-d)). Furthermore, principal component is a vector that is perpendicular to one another which represent in for X, Y and Z-axis.

Meanwhile, Fig. 14 shows the correlation of a single spectrum at 1.0, 1.5 and 1.9 μm wavelengths with respect to the refractive index in the crystal holes. Based on the range of investigation, the gradient demonstrates the fact that a steeper curve at a wavelength of 1.0 μm will give the most sensitive sensor compared to 1.5 and 1.9 μm for un-tapered LMA-8. At 1.0 μm, the index change of 0.01 causing a large change in normalized power meanwhile at 1.9 μm, the index change causes a small change in normalized power where sensitivity is ΔP over ΔN. ΔP denote as the rate of change of normalized power and ΔN is denoted as the refractive index change of LMA-8 crystal holes.

It is advisable to use the transmission spectrum with respect to 1.0 tapered size. This proved that the LMA-8 PCF works equally well in tapered or un-tapered condition. Fig. 13(d) shows the parabolic relationship obtained which act as the standard reference of how LMA-8 being as a sensor by first the

LMA-8 being transverse propagate, then we analyzed the crystal structure by using PCA, afterward the spectrum reading obtained is 1.355 which falls in between 1.35 and 1.36 line of parabolic relationship.

Table 3. The color indication and the value of refractive index change

Refractive Index	Legend
1.33	
1.34	
1.35	
1.36	
1.37	
1.38	
1.39	
1.40	
1.41	
1.42	
1.43	

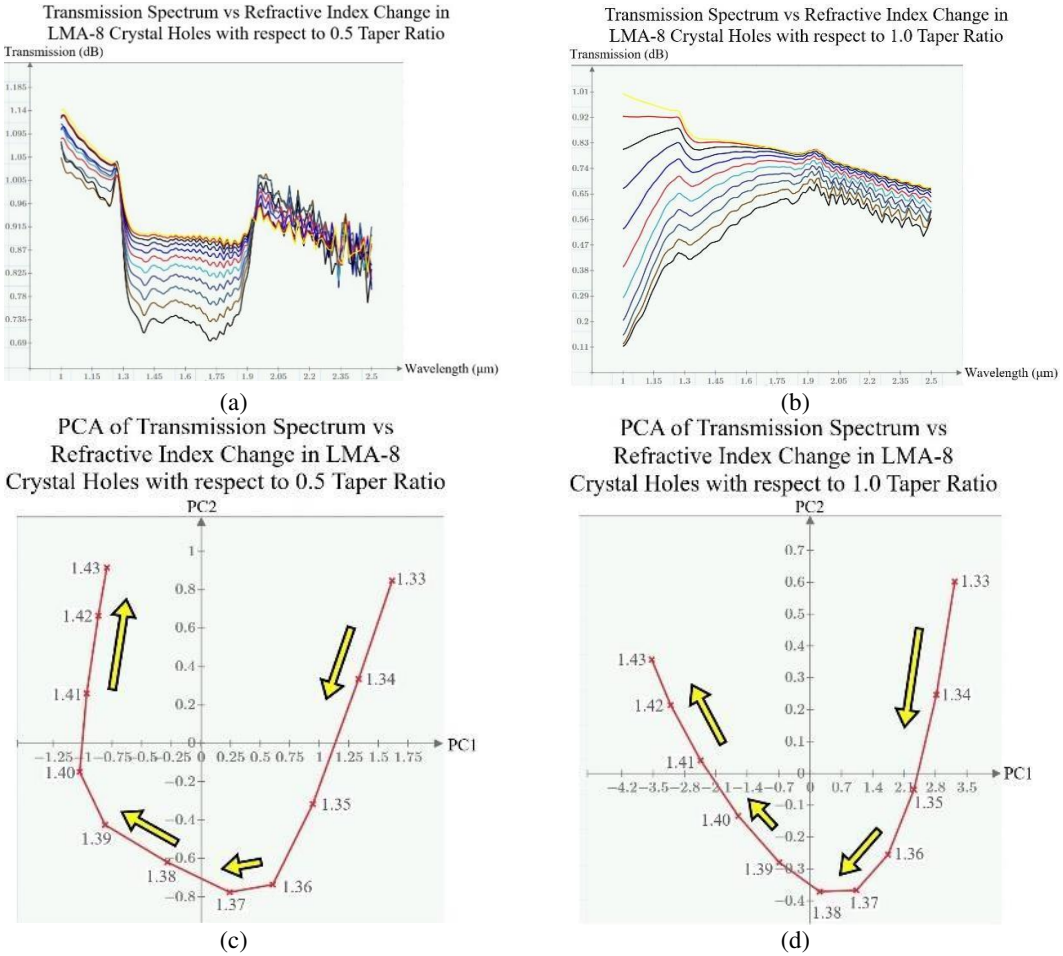

Figure 13: The transmission spectrum vs refractive index change in LMA-8 crystal holes with respect to (a) 0.5 taper ratio (b) 1.0 taper ratio and PCA of transmission spectrum for (c) 0.5 tapered (d) 1.0 tapered

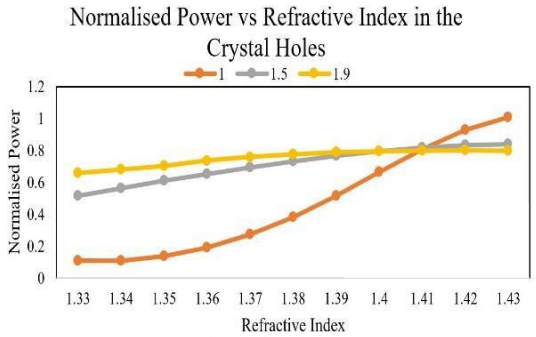

Figure 14: The correlation of a single spectrum at 1.0, 1.5 and 1.9 μm wavelength with respect to the refractive index in the crystal holes.

4. Conclusion and Recommendation

In summary, the advantage of scattering pattern and transverse transmission techniques is the capability to observe the diffraction pattern with light transverse and without having to cut the LMA-8 to destroy the sample. We have demonstrated that the scattering pattern is not a suitable technique to model the LMA-8 PCF as there is no relationship in pattern and uncluttered PCA with respect to taper ratio of 0.1 to 1.0 at 1.55 μm wavelength. This is because the LMA-8 fiber has bigger crystal size and bigger pitch size. Thus, this technique is more suitable to be applied when the crystal size is very small. As for the analysis of the transmission spectrum, there is a relationship between the transmission spectra and taper ratio of 0.1 and 1.0 at a range of 1.0 to 2.5 μm wavelength. Hence, this technique can be used to observe the difference in taper size. We proved that the LMA-8 PCF works equally well in tapered or un- tapered condition for the correlation of the transmission spectrum against the refractive index change from 1.33 to 1.43 in LMA-8 crystal holes. As a conclusion, this is a totally new research to be investigated and would produce interesting findings.

Acknowledgement

This work was partly supported by the Faculty of Electrical Engineering, Universiti Teknologi Mara Malaysia, and Ministry of Higher Education, Malaysia (research grant #FRGS/1/2015/TK04/UITM/03/5).

References

[1] J. D. Joannopoulos, R. D. Meade, and J. N.Winn, *Photonic Crystals* (Princeton University Press, Princeton, New Jersey 1995).
[2] J. D. Joannopoulos, P. R. Villeneuve, and S. Fan, "Photonic crystals: putting a new twist on light," Nature (London) 386, 143-149 (1997).
[3] K. Sakoda, *Optical Properties of Photonic Crystals* (Springer, Berlin 2001).
[4] M. M. Sigalas, R. Biswas, K. M. Ho, and C. M. Soukoulis, "Theoretical investigation of off-plane propagation of electromagnetic waves in two- dimensional photonic crystals," Phys. Rev. B **58**, 6791-6794 (1998).
[5] Z. Y. Li and Y. Xia, "Omnidirectional absolute band gaps in two- dimensional photonic crystals," Phys. Rev. B **64**, 153108 (2001).
[6] A. J. Ward and J. B. Pendry, "Calculating photonic Green's functions using a nonorthogonal finite-difference time-domain method," Phys. Rev. B **58**, 7252-7259 (1998).
[7] H. Y. D. Yang, "Finite difference analysis of 2-D photonic crystals," IEEE Trans. Microwave Theory Tech. **44**, 2688-2695 (1996).
[8] C. T. Chan, Q. L. Yu, and K. M. Ho, "Order-N spectral method for electromagnetic waves," Phys. Rev. B **51**, 16635-16642 (1995).
[9] A. Yariv and P. Yeh, *Optical Waves in Crystals* (Wiley, New York 1984).
[10] C. Kittel, Introduction to Solid State Physics (Wiley, New York 1976).
[11] T. A. Birks et al., "Full 2-D photonic bandgaps in silica/air structures", Electron. Lett., vol. 31, pp. 1941–1945, 1995.
[12] T.A. Birks, J.C. Knight, and P.St.J. Russell, "Endlessely single mode photonic crystal fiber," Opt. Lett.,

vol. 22, pp. 961-963, (1997).
[13] Philip St J. Russell, "Photonic-Crystal Fibers," J. Lightwave Technol.,vol. 24, pp. 4729-4749, (2006).
[14] J.C. Knight, T.A. Birks, P.St.J. Russell, and D.M. Atkin, "All silica single-mode optical fiber with photonic crystal cladding," Opt. Lett., vol.21, pp. 1547-1549, (1996).
[15] J.C. Knight, T.A. Birks, P.St.J. Russell, and J.P. Sandro, "Properties of photonic crystal fiber and the effective index model," J. Opt. Soc. Am. A, vol. 15, pp. 748-752, (1998).
[16] "Tutorial: Fiber Optic Basics." *Fiber Optic Basics*. Web. 27 May 2016.
[17] J. Arriaga, J.C. Knight, and P.St. Russell, "Modeling Photonic Crystal Fibers", Physica E 17, Elsevier Science, pp. 440-442, 2003.
[18] S. Soussi, "Modeling Photonic Crystal Fibers, Applied Mathematics", Elsevier Science, vol.36,Issue 3,pp.288- 317, 2006.
[19] M. D. Nielsen, N. A. Mortensen, and J. R. Folkenberg, "Reduced microdeformation attenuation in large-mode area photonic crystal fibers for visible applications," Opt. Lett. 28, 1645–1647 (2003).
[20] Colombe, Yves, Daniel H. Slichter, Andrew C. Wilson, Dietrich Leibfried, and David J. Wineland. "Single-mode Optical Fiber for High- power, Low-loss UV Transmission." *Opt. Express Optics Express* 22.16 (2014): 19783. Web.
[21] Szustakowski, M., N. Palka, and W. Grabiec. "Simple Method for Determination of Photonic Crystal Fibers Geometry." *Photonic Crystal Fibers* (2007).
[22] Sharma, Dinesh Kumar, and Anurag Sharma. "Spot Size of Photonic Crystal Fibers: An Analytical Method of Calculation." *2012 International Conference on Optical Engineering (ICOE)* (2012).
[23] Nielsen, M. D., J. R. Folkenberg, N. A. Mortensen, and A. Bjarklev. "Bandwidth Comparison of Photonic Crystal Fibers and Conventional Single-mode Fibers." *Opt. Express Optics Express* 12.3 (2004): 430.
[24] T.A. Birks, Y.W. Li, J. Lightwave Technol. **10**, 432 (1992).
[25] Nguyen, Hong C., Boris T. Kuhlmey, Eric C. Magi, Michael J. Steel, Cameron L. Smith, and Benjamin J. Eggleton. "Tapered Photonic Crystal Fibres: Properties, Characterisation, and Applications (Invited Paper)." *Photonic Materials, Devices, and Applications* (2005).
[26] E.C. Magi, P. Steinvurzel, B.J. Eggleton, J. Appl. Phys. **96**, 3976 (2004).
[27] J.C. Jasapara, Opt. Express **13**, 1228 (2005).
[28] H.C. Nguyen, P. Domachuk, B.J. Eggleton, M.J. Steel, M. Straub,M. Gu, M. Sumetsky, Opt. Express **12**, 1528 (2004).
[29] E.C. Magi, P. Steinvurzel, B.J. Eggleton, J. Appl. Phys. **96**, 3976 (2004). [30] "Principal Component Analysis Explained Visually." *Explained Visually*. Web. 28 May 2016.